AFRL-RX-WP-JA-2018-0137

ORIGAMI MECHANOLOGIC (POSTPRINT)

B.E. Trembl, Philip R. Buskohl, and Richard A. Vaia

AFRL/RX

Andrew S. Gillman

UES, Inc.

21 FEBRUARY 2018
Interim Report

Distribution Statement A.
Approved for public release: distribution unlimited.

(STINFO COPY)

AIR FORCE RESEARCH LABORATORY
MATERIALS AND MANUFACTURING DIRECTORATE
WRIGHT-PATTERSON AIR FORCE BASE, OH 45433-7750
AIR FORCE MATERIEL COMMAND
UNITED STATES AIR FORCE

REPORT DOCUMENTATION PAGE

Form Approved
OMB No. 0704-0188

1. REPORT DATE *(DD-MM-YY)*
21 February 2018

2. REPORT TYPE
Interim

3. DATES COVERED *(From - To)*
8 September 2014 – 21 January 2018

4. TITLE AND SUBTITLE
ORIGAMI MECHANOLOGIC (POSTPRINT)

5a. CONTRACT NUMBER
FA8650-15-D-5405-0002

5b. GRANT NUMBER

5c. PROGRAM ELEMENT NUMBER
62102F

6. AUTHOR(S)
1)) B.E. Trembl, Philip R. Buskohl, and Richard A. Vaia – AFRL/RX
2) Andrew S. Gillman – UES, Inc.
.

5d. PROJECT NUMBER
4348

5e. TASK NUMBER 0002

5f. WORK UNIT NUMBER
X0YE

7. PERFORMING ORGANIZATION NAME(S) AND ADDRESS(ES)

1) AFRL/RX
Wright-Patterson AFB
Dayton, OH 45433

2) UES, Inc.
4401 Dayton-Xenia Rd.
Dayton, OH 45432

8. PERFORMING ORGANIZATION REPORT NUMBER

9. SPONSORING/MONITORING AGENCY NAME(S) AND ADDRESS(ES)

Air Force Research Laboratory
Materials and Manufacturing Directorate
Wright-Patterson Air Force Base, OH 45433-7750
Air Force Materiel Command
United States Air Force

10. SPONSORING/MONITORING AGENCY ACRONYM(S)
AFRL/RXAS

11. SPONSORING/MONITORING AGENCY REPORT NUMBER(S)
AFRL-RX-WP-JA-2018-0137

12. DISTRIBUTION/AVAILABILITY STATEMENT
Distribution Statement A. Approved for public release: distribution unlimited.

13. SUPPLEMENTARY NOTES
PA Case Number: 88ABW-2018-0810; Clearance Date: 21 Feb 2018. This document contains color. Journal article published in Proceedings of the National Academy of Sciences of the United States of America), Vol. 115, No. 27, 18 June 2018. No copyright – open access. The U.S. Government is joint author of the work and has the right to use, modify, reproduce, release, perform, display, or disclose the work.
The final publication is available at www.pnas.org/cgi/doi/10.1073/pnas.1805122115

14. ABSTRACT *(Maximum 200 words)*
Robots autonomously interact with their environment through a continual sense–decide–respond control loop. Most commonly, the decide step occurs in a central processing unit; however, the stiffness mismatch between rigid electronics and the compliant bodies of soft robots can impede integration of these systems. We develop a framework for programmable mechanical computation embedded into the structure of soft robots that can augment conventional digital electronic control schemes. Using an origami waterbomb as an experimental platform, we demonstrate a 1-bit mechanical storage device that writes, erases, and rewrites itself in response to a timevarying environmental signal. Further, we show that mechanical coupling between connected origami units can be used to program the behavior of a mechanical bit, produce logic gates such as AND, OR, and three input majority gates, and transmit signals between mechanologic gates. Embedded mechanologic provides a route to add autonomy and intelligence in soft robots and machines.

15. SUBJECT TERMS
Origami folding; convex objective function; Chomper; Square Twist; facet bending and stretching; bifurcation

16. SECURITY CLASSIFICATION OF:

a. REPORT	b. ABSTRACT	c. THIS PAGE	17. LIMITATION OF ABSTRACT:	18. NUMBER OF PAGES
Unclassified	Unclassified	Unclassified	SAR	8

19a. NAME OF RESPONSIBLE PERSON (Monitor)
Lawrence Brott

19b. TELEPHONE NUMBER *(Include Area Code)*
(937) 255-9157

Origami mechanologic

Benjamin Treml[a], Andrew Gillman[a,b], Philip Buskohl[a], and Richard Vaia[a,1]

[a]Functional Materials Division, Materials and Manufacturing Directorate, Air Force Research Laboratory, Wright-Patterson Air Force Base, OH 45433; and [b]UES, Inc., Dayton, OH 45432

Edited by John A. Rogers, Northwestern University, Evanston, IL, and approved May 15, 2018 (received for review March 23, 2018)

Robots autonomously interact with their environment through a continual sense–decide–respond control loop. Most commonly, the decide step occurs in a central processing unit; however, the stiffness mismatch between rigid electronics and the compliant bodies of soft robots can impede integration of these systems. We develop a framework for programmable mechanical computation embedded into the structure of soft robots that can augment conventional digital electronic control schemes. Using an origami waterbomb as an experimental platform, we demonstrate a 1-bit mechanical storage device that writes, erases, and rewrites itself in response to a time-varying environmental signal. Further, we show that mechanical coupling between connected origami units can be used to program the behavior of a mechanical bit, produce logic gates such as AND, OR, and three input majority gates, and transmit signals between mechanologic gates. Embedded mechanologic provides a route to add autonomy and intelligence in soft robots and machines.

origami | soft robotics | logic | active materials

Robots are distinguished from machines on the basis of their autonomy. The most successful robots, such as manufacturing robots (1), the Mars rover, or Big Dog (2), use onboard computers as a coordinating intelligence and are mechanically robust to support the technological ecosystem associated with digital electronics. For soft robotics, with applications in assisted surgery (3), disaster response, and human rehabilitation and augmentation (4), mechanical constraints may limit the integration of electronic components throughout soft structures, so there is a need for alternative methods of incorporating computational abilities into soft robots. Mechanical logic devices have a long history, dating back to Leibniz's step reckoner in 1672 and Babbage's difference engine in 1822 (5), but hard mechanologic devices make use of gears, wheels, microelectromechanical systems (MEMS) (6), and even Legos to perform calculations. However, these approaches do not easily integrate with compliant machines.

Conventional electronic control of soft robots can be complemented by soft mechanologic, where the inputs and outputs are mechanical deformations of the robot's structural framework, distributed throughout a soft robot's body, and perform morphological computation locally, rather than passing all signals to a central processing unit (7, 8). This approach takes inspiration from animals, especially the octopus, which have distributed nervous systems in their limbs not only to carry signals to a coordinating intelligence (i.e., brain) but also to act reflexively (9). This work develops basic mechanologic units using origami as a platform. Bistable waterbomb origami structures serve as mechanical memory units. Incorporation of environmentally responsive soft materials that autonomously sense the local environment and transduce external signals into mechanical inputs produces composites that write, erase, and rewrite the mechanical bit without any external power supply. We show that mechanical coupling between origami units transfers information and enables creation of mechanical logic gates that can be connected to form reprogrammable mechanologic circuits. The fundamental building blocks of an origami-based soft mechanologic system demonstrated here provide a platform for further development and integration of distributed logic and reflexes into soft robots and machines.

Components of Mechanologic

Logic embedded into the structure of a soft robot is unlikely to replace the speed and information density of electronic logic; rather, electronic and mechanical logic will cooperate to control a robot. To develop mechanologic compatible with electronic logic, we seek to emulate the language and structure of electronic digital logic. This requires a mechanical bit to store information, logic gates to operate on stored information, signal transmission mechanisms to connect logic gates, and an ecosystem of sensors that interface with mechanical inputs. These components must operate on an energy budget that can be harvested from the environment. A few components, such as signal transmission (10), energy-harvesting sensors (11–13), and logic gates (14, 15) have been demonstrated individually. However, before a complete soft mechanological system can be established the components must be proven and integrated within a common platform.

Here, we demonstrate origami as a platform capable of integrating these components into a mechanologic system. Origami actuators have shown significant utility in the microrobotics community, due to their precise motion control and amenability to 2D fabrication techniques (16, 17). Origami patterns are modular (18), enabling units to be developed independently and combined to create more complicated functional structures. In addition, localization of deformation to the fold lines mechanically protects the facets, providing regions that can host electronic hardware. Advances in analyzing the nonlinear mechanics of origami have broadened the design space to include prediction of stable configurations, in addition to analysis of the fold path (19–21). Because origami patterns are scale-independent, insights into the mechanics, design, and implementation of origami mechanologic can be shared among disciplines, ranging from MEMS to deployable structures, that exploit origami mechanisms.

Significance

Autonomy separates robots from machines. Incorporating autonomy into soft robots is an outstanding challenge due to the mismatch between rigid electronics and the compliant bodies. In this work, we demonstrate origami as a platform for compliant mechanical logic, containing mechanical bits, logic gates, and signal transmission mechanisms that can supplement conventional electronic controls. Furthermore, these processes can be responsive to and programmed by the environment via the integration of adaptive materials. Thus, origami provides a framework in which sensing, computation, and reflexes can be seamlessly integrated into the compliant bodies of soft robotics.

Author contributions: P.B. and R.V. designed research; B.T. and A.G. performed research; B.T. and A.G. analyzed data; and B.T., A.G., P.B., and R.V. wrote the paper.

The authors declare no conflict of interest.

This article is a PNAS Direct Submission.

[1]To whom correspondence should be addressed. Email: richard.vaia@us.af.mil.

This article contains supporting information online at www.pnas.org/lookup/suppl/doi:10.1073/pnas.1805122115/-/DCSupplemental.

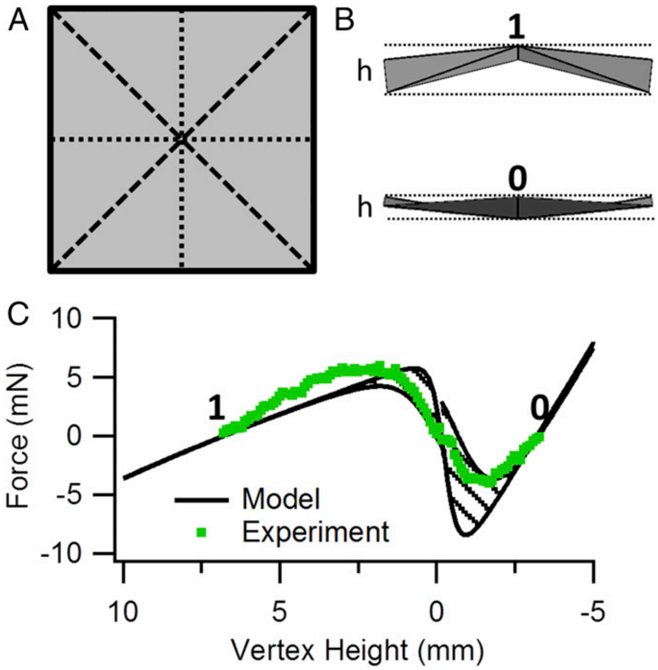

Fig. 1. Bistable origami mechanomemory. (*A*) Fold pattern for a waterbomb; dotted lines indicate mountain folds and dashed lines indicate valley folds. (*B*) The 1 and 0 states of the waterbomb base, with the vertex height (h) on each structure indicated. (*C*) Mechanics of the snap-through reconfiguration. The hatched region indicates the range of calculated force-displacement curves due to an estimation of the effective truss width in the governing equations. Green dots indicate the measured mechanical response of a polypropylene waterbomb.

Satisfying an origami axiom for flat folding has been interpreted as a mechanical logic problem, with mountain and valley assignment of a fold line as the mechanical 1 and 0 states (22). However, once folded these patterns are not dynamic or reprogrammable because there is only one set of mountain–valley assignments compatible with flat folding; any attempt to change a mountain to valley (1 to 0) leads to mechanical frustration. To produce dynamic mechanologic, the base unit must be able to switch between mechanical states without frustrating the system. Several bistable origami patterns have been identified (20, 23, 24) which may satisfy this criteria. Here, we focus on the waterbomb base fold pattern as a testbed because it serves as a model for the general bistability of origami vertices undergoing a vertex inversion process (24) and is a common motif found in more complicated origami structures (25). Fig. 1*A* shows the fold pattern for a waterbomb, as well as a model of the structure in its two stable configurations in Fig. 1*B*. During reconfiguration between stable states, the mountain and valley folds stay mountain and valley folds and the structure undergoes only a small change in projected area. We believe these properties allow the mechanical bit to switch between 1 and 0 states without interfering with the ability of other connected units to reconfigure in the multiunit structures presented below.

Fig. 1*C* shows measured and calculated force-displacement profiles of a waterbomb as a point load is applied to the vertex of the structure driving reconfiguration. The waterbomb is folded from a 40-μm-thick, 4 × 4-cm square film of polypropylene (PP), with a mass of about 60 mg. The waterbomb is modeled as a truss system following the work of Schenk and Guest (26) using the nonlinear formulation developed by Gillman et al. (19, 27). The model is comprised of truss elements that form triangular origami facets, with a torsional spring added to fold lines to account for the stiffness of an origami fold, as illustrated in *SI Appendix*, Fig. S3. The internal energy of a single truss element is given by

$$U = l_0 \int_0^1 \frac{EA}{2}\,\varepsilon^2 + \frac{G}{2}\,\tilde{\varphi}^2 \; d\,\zeta,$$

where l_0 is the initial length of the truss, E is the Young's modulus (3 GPa), A is the cross-sectional area of the truss, G is the fold stiffness ($2{\cdot}10^{-3}$ N·m/m), ε is the axial strain in the truss, and $\tilde{\varphi}$ is the rotation of the torsional spring. The first term represents axial strain in the truss elements and accounts for facet stretching, while the second term represents energy stored in the torsional spring emanating from bending/folding. See *SI Appendix, Supplemental Note 2* for additional details of this model. The unit waterbomb structure presented in Fig. 1 is composed of 16 truss elements (solid and dashed lines in Fig. 1*A*), 8 of which correspond to folds (dashed lines in Fig. 1*A*) and are modeled with nonzero fold stiffness G. The fold stiffness is measured from the force displacement behavior of a single PP fold (*SI Appendix*, Fig. S9), while the Young's modulus is taken from the manufacturer's data sheet. The cross-sectional area term is the product of the film thickness (40 μm) and an effective truss width. This width is the only adjustable parameter in the calculations. The dependence of the force-displacement curve on the truss width parameter decreases away from the snap-through event, indicating folding dominated deformation. For a range of reasonable values (0.6–2 cm) for this parameter, peak forces and the absorbed energy during reconfiguration are within 30% of the measured values with the exception of the peak force involved in snapping from 0 to 1, which is overestimated by up to 110%. A truss width of 0.6 cm is used for all further calculations. Good agreement between the experimentally measured origami mechanics and a simple model aids the design and analysis of the mechanologic devices presented below.

To produce a sense–decide–respond loop in an origami bit, there is a need for materials that can respond to external stimuli and harvest energy to write and erase the mechanical memory. The field of responsive soft materials provides a suite of materials capable of harvesting energy from the environment and transducing environmental signals into mechanical responses. A wide variety of materials have been developed that respond to a range of stimuli such as heat, light, magnetism, and humidity (28, 29). In this work, we use a humidity responsive polymer, poly(3,4-ethylenedioxythiophene) polystyrene sulfonate (PEDOT:PSS) as a prototype responsive soft material. PEDOT:PSS is a conductive polymer commonly used in flexible and organic electronics. PEDOT:PSS transduces a relative humidity (RH) change into a mechanical response. Upon absorption and desorption of water vapor, PEDOT:PSS will swell and shrink, generating up to 4% strain (30). The conductivity and hygromechanical response of PEDOT:PSS provides a route to interface between mechanologic distributed throughout the structure of a soft robot and conventional electronic controls. The mechanical response of a composite of 24-μm-thick PEDOT:PSS on a 40-μm-thick PP film follows bilayer bending mechanics, as predicted by Timoshenko (31) (*SI Appendix, Supplemental Note 1*), indicating that continuum approximations will be sufficient to predict the motion of origami structures with distributed PEDOT:PSS transducers.

We demonstrate environmental responsivity and energy harvesting, mechanical state change, and fidelity of our nonlinear truss model in Fig. 2. Placing PEDOT:PSS transducers at the fold lines allows for validation of our origami model using a different loading condition than was used for calibration in Fig. 1. Depending on the location of the active material (outside vs. inside of folds), the bending moment applied by the PEDOT:PSS can either open or close the folds. Representative images of the waterbomb are shown in Fig. 2 *A–D*, during both fold closing (B → A) and fold opening

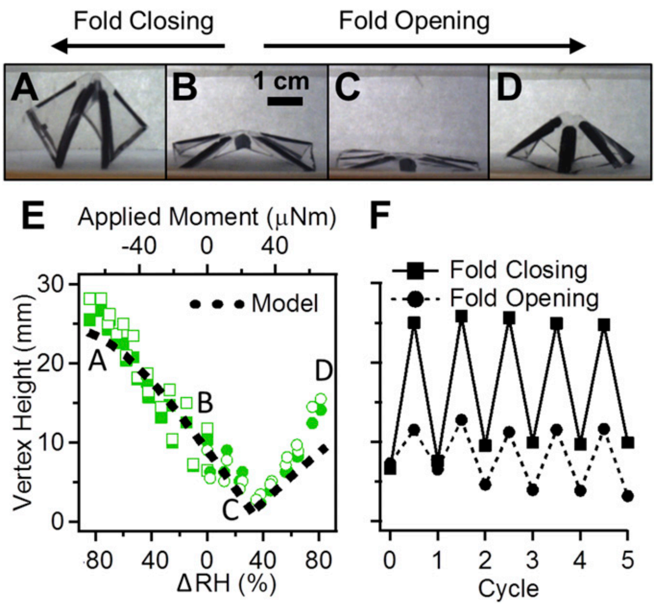

Fig. 2. Environmental sensing and actuation of origami. (*A*–*D*) Reconfiguration of waterbombs with PEDOT:PSS actuators on the inside (*A* and *B*) and outside (*C* and *D*) of fold lines. B is the equilibrium configuration which transforms into A, C, or D upon a change in the RH. All images are at the same scale. (*E*) Change in the height of the vertex as the RH is reduced from an initial value of 85%. Letters indicate where the configurations shown in *A*–*D* occur. Squares indicate samples that undergo fold closing and circles indicate samples that undergo fold opening and inversion. Filled and open symbols indicate separate waterbomb samples. The dotted black line is a calculated vertex height using the nonlinear truss model. (*F*) Cycling of waterbombs between states B and A and states B and D repeatedly. Half cycles are the reconfigured structure, A or D, while whole cycles are the stress-free state, B.

(B → C → D) transitions. Applying distributed bending moments to the fold lines is a unique way to load an origami structure that would be difficult to produce with conventional mechanical testing equipment. As a result, the fold closing and opening reconfigurations demonstrated here have not, to the best of our knowledge, been studied previously. Fig. 2*E* compares the observed reconfiguration of the structure to our origami model with bending moments applied to the fold lines. Using the stress-free state (B) and the flat state (C) to provide a scaling factor between the humidity-driven experimental structure and our origami model, we see good agreement between the calculated and experimentally observed origami mechanics. After an initial change in the stress-free configuration likely due to plastic deformation in the folds, the structure can undergo this actuation cycle repeatedly, as shown in Fig. 2*F*.

The continuous relationship between humidity-driven bending at the folds and linear actuation of the vertex is an analog-to-analog transduction of an environmental input into a mechanical output. For a waterbomb, the mechanical output manifests itself as linear actuation of the vertex; however, changing the underlying origami structure will produce other mechanical responses such as twisting or large areal changes (20, 32). Recently, origami optimization routines have been developed that take a set of possible fold lines and develop an optimal fold pattern for a desired mechanical response (21). The integration of environmentally triggered distributed forces into the origami truss model shown here highlights the opportunity to simultaneously optimize both the fold pattern and actuator placement for the rational design of dynamic origami structures.

Mechanologic Units

The origami actuator in Fig. 2 transforms via a fold inversion mechanism, which may not be compatible with dynamic origami logic structures. Instead, we return to the vertex inversion reconfiguration presented in Fig. 1 to provide the mechanical 1 and 0 states. The simplest logic gates take two inputs and compare them to produce an output following a simple set of rules. In Fig. 3, symmetric and antagonistic PEDOT:PSS transducers on the top and bottom of the waterbomb vertex sense their local environment, transduce the environmental stimulus into a mechanical input, and compare them via a force balance at the vertex. If the waterbomb is in a uniform RH environment, both actuators sense and respond to the same signal, producing no net force and no change to the origami structure. However, in an RH gradient the PP layer restricts diffusion of water vapor, forcing it to diffuse around rather than through a waterbomb. As a result, the top and bottom sensors detect significantly different local environments as shown in Fig. 3*A*. The PEDOT:PSS actuator exposed to a lower RH exerts a larger force on the vertex, bending the origami structure and, depending on the initial waterbomb state, reconfiguring the structure.

Adding environmentally responsive actuators to a mechanical bit elevates the composite structure from a mechanical memory unit to an environmentally responsive logic gate. If we digitize the signals sent to the top and bottom actuator as just high (1) and low (0) RH and the two vertex configurations as 1 and 0, then a waterbomb with a pair of antagonistic actuators at the vertex acts as a mechanical version of the logic gate known as an SR latch. The SR latch is the fundamental logic gate for sequential digital logic (33). More precisely, because PEDOT:PSS exerts no force in response to environmental 1, and compressive force in response to environmental 0, PEDOT:PSS acts as a

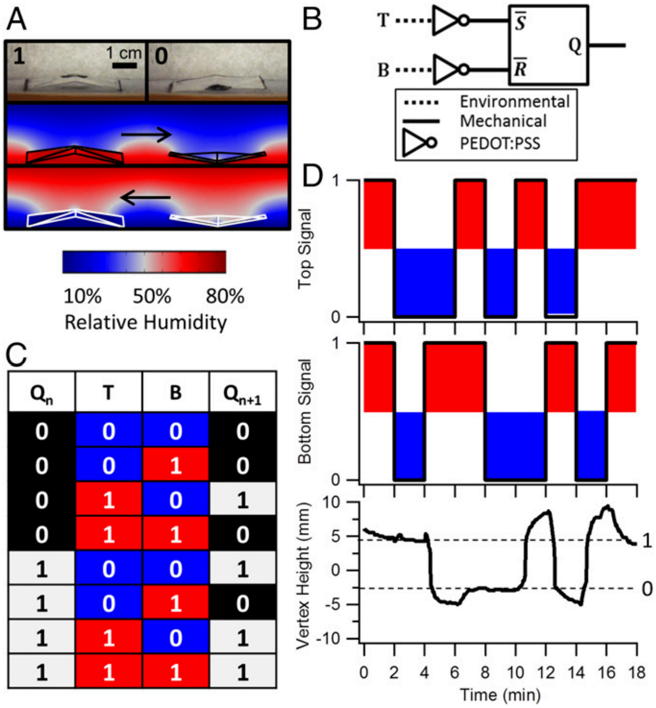

Q_n	T	B	Q_{n+1}
0	0	0	0
0	0	1	0
0	1	0	1
0	1	1	0
1	0	0	1
1	0	1	0
1	1	0	1
1	1	1	1

Fig. 3. A mechanical SR latch. (*A*) A waterbomb with actuators at the vertex switches between 1 and 0 in response to a vertical humidity gradient. Steady-state COMSOL simulations show the RH distribution around a waterbomb. (*B*) Symbolic representation of the SR latch, where environmental signals (dotted lines) are transduced to mechanical signals (solid lines) by PEDOT:PSS. (*C*) State transition table for a waterbomb. T and B indicate the environmental signal detected by the top and bottom actuator, respectively. Q is the state of the mechanical bit (vertex up or down). (*D*) An environmentally responsive waterbomb writes, erases, and rewrites itself in response to time varying environmental stimuli. The dotted lines indicate the equilibrium configuration of the 1 and 0 states.

NOT gate that senses and transduces an environmental input into a mechanical input. These mechanical inputs on the top and bottom of the vertex are the Set ($\bar{S}$) and Reset ($\bar{R}$) signals for the $\overline{SR}$ latch, which has the mechanical output (Q) of either the 1 or 0 state of the waterbomb structure. Fig. 3*B* shows a symbolic representation of the mechanologic device. The state transition table of the device is shown in Fig. 3*C*; Q_n indicates the current state of the waterbomb (vertex up = 1, white and vertex down = 0, black), the environmental inputs into the structure, the humidity at the top (T) and bottom (B) actuators are colored to match the color scale of the simulated humidity distribution in Fig. 3*A*, and Q_{n+1} indicates the subsequent state after sensing and responding to the environment. Fig. 3*D* shows the response of a waterbomb to a time-varying environmental stimulus; the waterbomb writes, erases, and rewrites itself by snapping between the 1 and 0 states in response to the external environment, following the rules of its state transition table. Video of this experiment is available in Movie S1. In addition to serving as a mechanological memory unit, the environmental energy harvesting of the PEDOT:PSS actuators, combined with the structural energy storage and rapid release during snap-through, can be exploited to drive autonomous locomotion, as demonstrated in Movie S3 and *SI Appendix*, *Supplemental Note 4*.

Mechanologic Gates and Circuits

Complex logic circuits for sensing, memory, and computation are built from logic gates that perform simple Boolean operations such as AND, OR, and NOT. In electronic logic, logic gates manipulate input voltages to produce an output voltage, which is carried to other gates by wires. Mechanologic uses a mechanical state to encode a 1 or 0, and so the inputs to and outputs of a mechanologic gate must likewise be mechanical. In Fig. 4, we explore mechanical coupling between waterbomb units as a means of building Boolean mechanologic gates. Fold patterns for connecting one to four waterbombs to a central device unit are shown in Fig. 4*A*. Smaller schematics enumerate all possible combinations of states of the coupled waterbombs and are labeled using binary notation starting from the left and moving clockwise around the central gray unit (white = 1, black = 0). For example, a 5mer with the waterbombs in the one and three positions snapped through is labeled 0101. The details of constructing and modeling these complex origami structures are discussed in *SI Appendix*, *Supplemental Note 2*. Each waterbomb in a network could be triggered by a different stimulus, thus providing a means to consolidate different environmental stimuli to a decision point.

Connected waterbomb units share a fold line and two facets that serve to communicate the mechanical state of a waterbomb to its neighbor. The essentials of mechanical coupling between connected waterbombs can be seen in the 2mer (Fig. 4*B*). When a connected waterbomb is in the 1 state, reconfiguration of the central waterbomb becomes more difficult because opening of the shared fold between the waterbombs is resisted by the connected waterbomb. The result is an increase in the energetic barrier to snap-through of 11.6 μJ (33%) relative to a 1mer. In contrast, when a connected waterbomb is a 0, the shared fold is held open relative to an isolated waterbomb, as the 0 state has a less folded equilibrium state, and reduces the barrier to reconfiguration by 5.1 μJ (15%). Fig. 4*C* summarizes the effect of connecting additional waterbombs and snapping connected waterbombs between 1 and 0 states on the energetic barrier to reconfiguration of the central device unit for all of the fold patterns and configurations in Fig. 4*A*. To the first order, increasing the number of connected waterbombs in a 1 state linearly increases the energetic barrier to snap-through of the central waterbomb (14 μJ per connected waterbomb), while snapping a connected waterbomb from 1 to 0 linearly decreases the barrier to reconfiguration (17 μJ per snapped waterbomb). When two connected waterbombs are 0s, the barrier to snap through varies by about 3 μJ depending upon whether the 0s are next to or across from each other; for example, consider the 001 vs. 010 configurations of a 4mer.

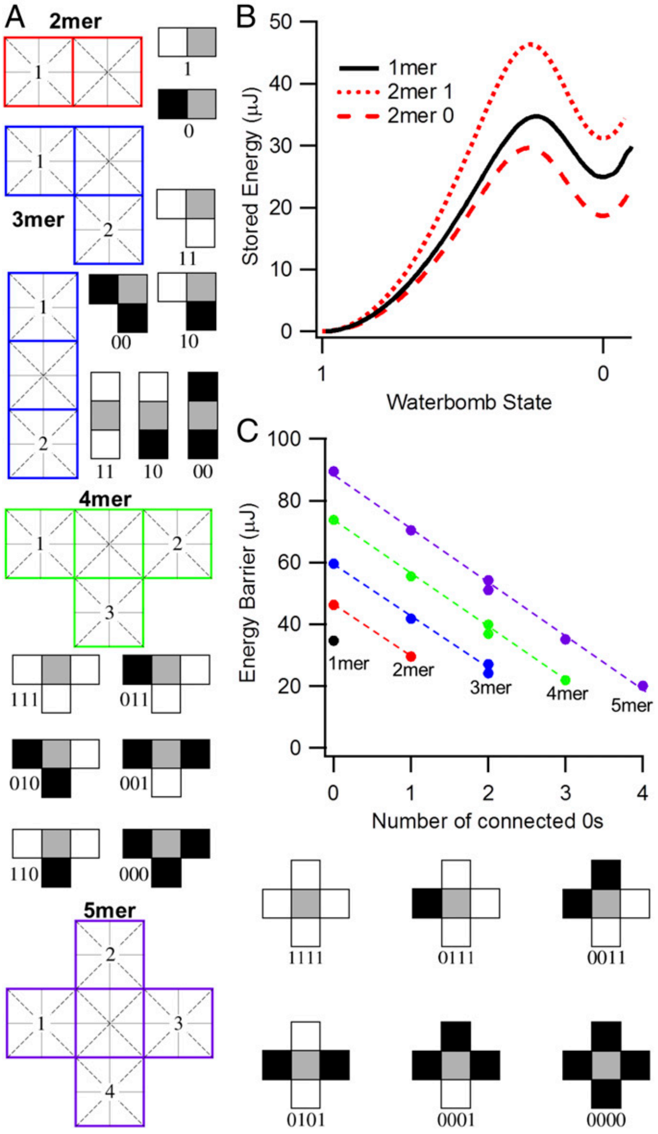

Fig. 4. Mechanical coupling in origami. (*A*) Fold patterns (colored) and possible states (black and white) of all possible nearest-neighbor coupled waterbombs. Numbers in adjacent waterbombs indicate the order that states are listed in when labeled. White indicates waterbombs in the 1 state, black indicates waterbombs in the 0 state, and gray indicates the central device unit for which the mechanics of snap-through are calculated. (*B*) Energy stored in the origami structure as the central waterbomb is reconfigured from 1 to 0. (*C*) Energetic barrier to reconfiguration for all waterbomb configurations shown in *A*. By snapping neighboring units from 1 to 0, the energetic barrier can be tuned across a wide range, which can be used to program the susceptibility of the central waterbomb.

The mechanical force applied by an embedded transducer, and hence energy transferred to a waterbomb unit, is constant for a set combination of responsive material and external stimulus. If we consider the mechanical state of connected waterbomb units as inputs that modulate the energetic barrier to reconfiguration of the central device unit, which serves as an output, the origami structures in Fig. 4*A* can be used to create mechanologic gates. Fig. 5*A* demonstrates an AND gate created from a linear 3mer with an environmentally sensitive actuator on only the center waterbomb. In a humidity gradient (T = 0, B = 1), the center

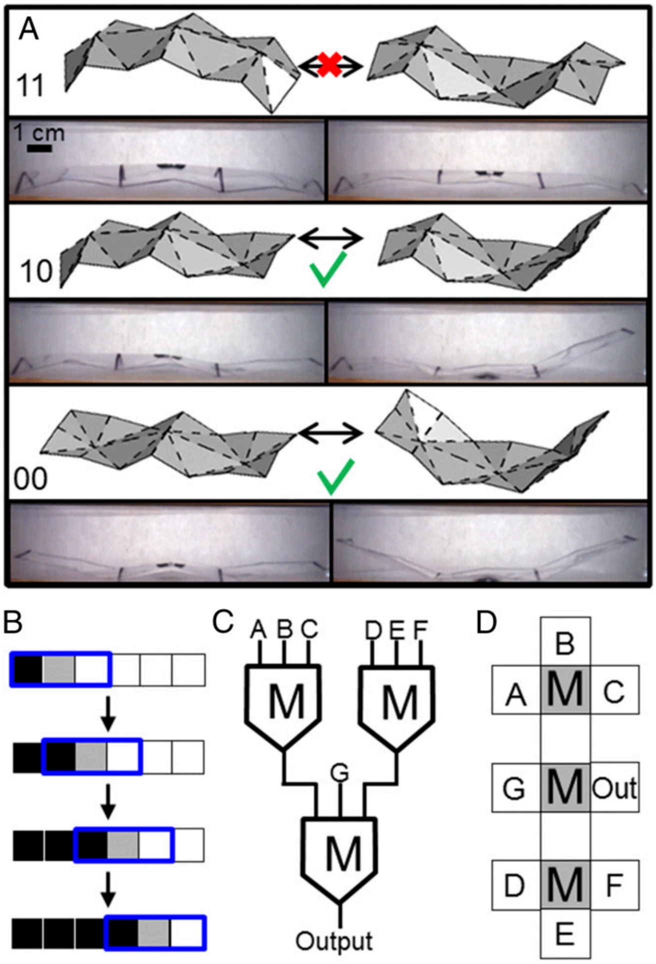

Fig. 5. Logic gates and signal transmission. (*A*) Models of the equilibrium states of a linear 3mer, along with corresponding photos of an experimental 3mer with PEDOT:PSS only at the center vertex. Photos on the left are at ambient conditions; photos on the right are in a T = 0, B = 1 environment. Snap-through does not occur for the 11 state (red x) because the energetic barrier to reconfiguration is too high. All images are at the same scale. (*B*) Sequential propagation of reconfiguration in a waterbomb chain. The blue box highlights a waterbomb that has the local mechanical environment of a 01 linear 3mer. When the light gray unit harvests energy from the environment and reconfigures, it alters the mechanical environment of its neighbor, resulting in signal propagation. (*C*) Abstract logic diagram for a seven-input reprogrammable logic circuit. (*D*) Implementation of the logic circuit shown in *C* using waterbomb-based mechanologic. Input and logic gate waterbombs are labeled A–G and M, respectively. Empty waterbombs act as wires as illustrated in *B*.

waterbomb is unable to snap through when coupled to two waterbombs in the 1 state due to the raised energetic barrier to reconfiguration. When one or both of the connected waterbombs is a 0, the energetic barrier is reduced below the output of the environmentally sensitive actuator and the center waterbomb snaps. The full state transition table for this origami logic gate is shown in *SI Appendix*, Table S1. Simultaneous control over the embedded actuator, which sets the threshold for reconfiguration, and the origami structure, which determines the number of inputs available, can be used to create a wide range of logic gates including AND, OR, and multiple input majority gates. Three input majority gates are of particular interest because when one input is used as a programming input they can be dynamically switched between performing AND and OR functions (34).

To connect logic gates together into a complex logic circuit, outputs of one logic gate must be transmitted to the input of another logic gate. As the mechanical coupling that modulates the barrier to snap-through is local, propagation of this signal over arbitrary distances is a challenge. Tiling of 3mer AND gates provides one route to address this issue via a sequential snap-through process. Fig. 5*B* schematically illustrates this process for a linear chain of waterbombs, assuming an environmental stimulus is present to provide the energy for snap-through (*SI Appendix*, *Supplemental Note 3* and Movies S4 and S5). An initially snapped-through waterbomb on the left side of a waterbomb "wire," which can be an externally programmed unit, sensor unit, or the central device unit of a previous logic gate, reduces the barrier to reconfiguration of its neighbor to the right. This waterbomb snaps through and lowers the energetic barrier for its neighbor, and so on down the line. The last unit of a waterbomb "wire" can then serve as an input unit to a mechanologic gate.

The waterbomb-based mechanologic system presented here is a mechanical implementation of 2D cellular automata (35). Quantum dot cellular automata (QDCA) have been studied extensively as an alternate to conventional field-effect transistor-based digital logic (34). Like our implementation of origami mechanologic, QDCA have a square unit cell and transfer local interactions through a logic circuit via sequential reconfiguration. Designs for complex logic circuits, including adders and multipliers, have been developed that may be adaptable to origami mechanologic (36, 37). For instance, if the transducer in the central waterbomb of a 5mer has a maximum energy input between 55 and 70 μJ and one connected waterbomb is reserved for transmitting the output, the 5mer will behave as a three-input majority gate. When three three-input majority gates are connected as shown in Fig. 5*C* the resulting seven input logic circuit leverages the programmability of three input majority gates to create a structure that can perform the four-input AND, four-input OR, sum-of-products, or product-of-sums operations (37). Fig. 5*D* diagrams a compact implementation of this structure in our mechanologic platform, where gray squares indicate the device units of the three-input majority gates. The unlabeled units between majority gates act as wires to transmit the output of the left and right gates to the central gate as discussed above.

Discussion

The demonstration of a mechanical bit, environmentally responsive transducers, logic gates, and a signal transmission mechanism in a single platform makes origami mechanologic a promising route to embed local computation and programmable reflexes into the structural framework of soft robots. While the experimental demonstrations in this work use only humidity-responsive actuators of a constant size, the environmental responsivity of a soft robot can be controlled at a unit by unit level by exploiting advances in additive manufacturing and the suite of stimuli-responsive materials to independently control stimuli measurement, signal propagation, and logic operations. In addition, integration of environmentally responsive logic into the structural framework of a soft robot means that even simple binary transitions not routed through a complex mechanologic circuit can have a large impact on the shape or mechanical properties of a soft robot's body, for example programmatically changing the compressive modulus of an origami sheet (38).

The implementation of mechanologic developed here is not without limitations. The set of Boolean logic gates accessible via the structures in Fig. 4 does not include a NOT, NAND, or NOR gate, all of which require the energetic barrier for reconfiguration to increase when a connected unit is snapped from 1 to 0, rather than decrease. Without one of these gates, the mechanologic system developed here is not functionally complete, meaning that logic circuits with arbitrary truth tables cannot be produced. Furthermore, the 2D nature of origami limits circuit design and fan out of outputs of a logic gate, as a central device unit can only have up to four total inputs and outputs. These limitations may be addressed through incorporation of other origami fold patterns or may be circumvented in mechanologic systems based on alternate bistable building blocks. The selection criteria for an origami mechanical bit as well as the rules for coupling units together to produce mechanical logic gates that have been developed here may transfer to the development of mechanologic in other bistable systems. However, it is likely that we have encountered only a subset of the criteria for a complete mechanologic system and that other mechanologic platforms have advantages and constraints not encountered in our study of a waterbomb-based mechanologic.

Ultimately, mechanologic cannot replace electronics and provide all controls for a soft robot. Instead, compliant mechanologic can be leveraged to augment and complement traditional robotic controls. Mechanologic provides an opportunity to reduce the complexity of mechanical structure control by embedding an environmentally powered sense–decide–respond loop locally in the structural framework. Significantly complex logic and long-term memory are best left to electronics, and the rigid facets of origami provide good places to mount electronic hardware. Advances in additive manufacturing of flexible electronics provide possibilities for interaction between conventional electronic controls and mechanologic, including transduction of an electrical stimulus into a mechanical response via joule heating of PEDOT:PSS (30) and transduction of a mechanical shape change into a resistance change of a flexible conductor (39).

Conclusions

In this work we have used the waterbomb-based origami structure combined with environmentally responsive PEDOT:PSS actuators to demonstrate how a system of digital mechanologic might be generated. We leverage the bistability of origami vertices to store information mechanically in the origami structures. Integration of environmentally responsive actuators into the origami structure enables autonomous sensing and transduction of an environmental signal into a mechanical signal, resulting in a self-powered mechanical $\overline{SR}$ latch. Mechanical coupling between origami units that share folds and facets enables the creation of Boolean mechanologic gates, signal transmission mechanisms, and complex mechanological circuits. The fundamental concepts demonstrated here, whether implemented using an origami mechanologic language or another form of morphological computation, provide a route to embedding reflexes and distributed intelligence in soft machines that will enable them to autonomously sense, respond to, and interact with their environment, thereby truly earning the title of soft robots.

Materials and Methods

Waterbomb samples were folded by hand from 40-μm-thick PP films. PEDOT:PSS was deposited onto the films via drop casting and patterned using the procedure detailed in the *SI Appendix*, Fig. S8. Humidity gradients were generated by a custom-built humidity chamber (see ref. 11 for details). Extended discussion of the truss-based origami model, experimental procedures, and additional demonstrations of environmentally responsive origami can be found in *SI Appendix* and Movies S1–S5.

ACKNOWLEDGMENTS. We thank Nathan Price for his help in some data collection. This research was completed at the Air Force Research Laboratory at Wright-Patterson Air Force Base with funding support from the Materials and Manufacturing Directorate (RX) and the Air Force Office of Scientific Research. B.T. acknowledges a National Research Council postdoctoral fellowship.

1. Pan Z, Polden J, Larkin N, Van Duin S, Norrish J (2012) Recent progress on programming methods for industrial robots. *Robot Comput-Integr Manuf* 28:87–94.
2. Raibert M, Blankespoor K, Nelson G, Playter R (2008) Bigdog, the rough-terrain quadruped robot. *IFAC Proc Vol* 41:10822–10825.
3. Sareh S, et al. (2014) Bio-inspired tactile sensor sleeve for surgical soft manipulators. *2014 IEEE International Conference on Robotics and Automation (ICRA),* (IEEE, Piscataway, NJ), pp 1454–1459.
4. Polygerinos P, Wang Z, Galloway KC, Wood RJ, Walsh CJ (2015) Soft robotic glove for combined assistance and at-home rehabilitation. *Robot Auton Syst* 73:135–143.
5. O'Regan G (2013) *Mathematics in Computing* (Springer, New York).
6. Mahboob I, Yamaguchi H (2008) Bit storage and bit flip operations in an electromechanical oscillator. *Nat Nanotechnol* 3:275–279.
7. Correll N, Önal ÇD, Liang H, Schoenfeld E, Rus D (2014) Soft autonomous materials—Using active elasticity and embedded distributed computation. *Experimental Robotics* (Springer, New York), pp 227–240.
8. McEvoy MA, Correll N (2015) Materials science. Materials that couple sensing, actuation, computation, and communication. *Science* 347:1261689.
9. Hague T, Florini M, Andrews PL (2013) Preliminary in vitro functional evidence for reflex responses to noxious stimuli in the arms of Octopus vulgaris. *J Exp Mar Biol Ecol* 447:100–105.
10. Raney JR, et al. (2016) Stable propagation of mechanical signals in soft media using stored elastic energy. *Proc Natl Acad Sci USA* 113:9722–9727.
11. Treml BE, et al. (2018) Autonomous motility of polymer films. *Adv Mater* 30:1705616.
12. Jochum FD, Theato P (2013) Temperature- and light-responsive smart polymer materials. *Chem Soc Rev* 42:7468–7483.
13. Shin B, et al. (2018) Hygrobot: A self-locomotive ratcheted actuator powered by environmental humidity. *Sci Robot* 3:eaar2629.
14. Ion A, Wall L, Kovacs R, Baudisch P (2017) Digital mechanical metamaterials. *Proceedings of the 2017 CHI Conference on Human Factors in Computing Systems,* (Assoc for Computing Machinery, New York), pp 977–988.
15. Mosadegh B, et al. (2010) Integrated elastomeric components for autonomous regulation of sequential and oscillatory flow switching in microfluidic devices. *Nat Phys* 6: 433–437.
16. Onal CD, Wood RJ, Rus D (2011) Towards printable robotics: Origami-inspired planar fabrication of three-dimensional mechanisms. *2011 IEEE International Conference on Robotics and Automation (ICRA),* (IEEE, Piscataway, NJ), pp 4608–4613.
17. Boyvat M, Koh J-S, Wood RJ (2017) Addressable wireless actuation for multijoint folding robots and devices. *Sci Robot* 2:eaan1544.
18. Mousanezhad D, Kamrava S, Vaziri A (2017) Origami-based building blocks for modular construction of foldable structures. *Sci Rep* 7:14792.
19. Gillman A, et al. (2017) Discovering origami fold patterns with optimal actuation through nonlinear mechanics analysis. *41st Mechanisms and Robotics Conference* (Am Soc Mechanical Engineers, New York), Vol 5B, p V05BT08A052.
20. Silverberg JL, et al. (2015) Origami structures with a critical transition to bistability arising from hidden degrees of freedom. *Nat Mater* 14:389–393.
21. Fuchi K, et al. (2015) Origami actuator design and networking through crease topology optimization. *J Mech Des* 137:091401.
22. Bern M, Hayes B (1996) The complexity of flat origami. *Proceedings of the Seventh Annual ACM-SIAM Symposium on Discrete Algorithms* (Soc for Industrial and Applied Mathematics, Philadelphia), pp 175–183.
23. Hanna BH, Lund JM, Lang RJ, Magleby SP, Howell LL (2014) Waterbomb base: A symmetric single-vertex bistable origami mechanism. *Smart Mater Struct* 23:094009.
24. Lechenault F, Adda-Bedia M (2015) Generic bistability in creased conical surfaces. *Phys Rev Lett* 115:235501.
25. Yasuda H, Chen Z, Yang J (2016) Multitransformable leaf-out origami with bistable behavior. *J Mech Robot* 8:031013.
26. Schenk M, Guest SD (2011) Origami folding: A structural engineering approach. Origami 5: *Fifth International Meeting of Origami Science, Mathematics, and Education*, eds Wang-Iverson P, Lang RL, Yim M (CRC Press, Boca Raton, FL), pp 291–304.
27. Gillman A, Fuchi K, Buskohl PR (May 17, 2018) Truss-based nonlinear mechanical analysis for origami structures exhibiting bifurcation and limit point instabilities. *Int J Solids Struct*, 10.1016/j.ijsolstr.2018.05.011.
28. Kempaiah R, Nie Z (2014) From nature to synthetic systems: Shape transformation in soft materials. *J Mater Chem B* 2:2357–2368.
29. Geryak R, Tsukruk VV (2014) Reconfigurable and actuating structures from soft materials. *Soft Matter* 10:1246–1263.
30. Okuzaki H, Suzuki H, Ito T (2009) Electrically driven PEDOT/PSS actuators. *Synth Met* 159:2233–2236.
31. Timoshenko S (1925) Analysis of bi-metal thermostats. *JOSA* 11:233–255.
32. Miura K (2009) The science of Miura-ori: A review. *Origami 4*, eds Lang RJ, Peters AK (CRC, Boca Raton, FL), pp 87–100.
33. Pedroni VA (2008) *Digital Electronics and Design with VHDL* (Morgan Kaufmann, Burlington, MA).
34. Amlani I, et al. (1999) Digital logic gate using quantum-dot cellular automata. *Science* 284:289–291.
35. Wolfram S (1984) Cellular automata as models of complexity. *Nature* 311:419.
36. Cho H, Swartzlander EE (2007) Adder designs and analyses for quantum-dot cellular automata. *IEEE Trans NanoTechnol* 6:374–383.
37. Townsend WJ, Abraham JA (2004) Complex gate implementations for quantum dot cellular automata. *Fourth IEEE Conference on Nanotechnology, 2004* (IEEE, Piscataway, NJ), pp 625–627.
38. Silverberg JL, et al. (2014) Applied origami. Using origami design principles to fold reprogrammable mechanical metamaterials. *Science* 345:647–650.
39. Valentine AD, et al. (2017) Hybrid 3D printing of soft electronics. *Adv Mater* 29: 1703817.